Dalton Transactions

Accepted Manuscript

This is an *Accepted Manuscript*, which has been through the Royal Society of Chemistry peer review process and has been accepted for publication.

Accepted Manuscripts are published online shortly after acceptance, before technical editing, formatting and proof reading. Using this free service, authors can make their results available to the community, in citable form, before we publish the edited article. We will replace this *Accepted Manuscript* with the edited and formatted *Advance Article* as soon as it is available.

You can find more information about *Accepted Manuscripts* in the Information for Authors.

ROYAL SOCIETY OF CHEMISTRY

www.rsc.org/dalton

Synthesis and structural characterization of Al-containing interlayer-expanded-MWW zeolite with high catalytic performance

Toshiyuki Yokoi*, Shun Mizuno, Hiroyuki Imai, and Takashi Tatsumi**

Chemical Resources Laboratory, Tokyo Institute of Technology, 4259 Nagatsuta, Midori-ku,Yokohama 226-8503, Japan

Corresponding authors:

Fax number: +81-45-924-5282,

*E-mail address: *yokoi.t.ab@m.titech.ac.jp, **ttatsumi@cat.res.titech.ac.jp*

Abstract

Treatment of the zeolitic layered precursor of Al-MWW, so-called Al-MWW(P), with diethoxydimethylsilane (DEDMS) in acidic media leads to the formation of an aluminosilicate-type interlayer-expanded zeolite MWW (Al-IEZ-MWW) with expanded 12-membered ring (12-MR) micropores. However, the silylation process under acidic conditions simultaneously causes dealumination from the **MWW** framework, resulting in the decrease in the acid amount. We have developed a method for preparing Al-IEZ-MWW without leaching of the Al species. The strategy is to conduct the silylation under weakly acidic conditions; the silylation was conducted in the aqueous solution of ammonium salt, *e.g.*, NH_4Cl, instead of HNO_3. Subsequent additional acid treatment led to the formation of Al-IEZ-MWW that shows a high catalytic performance in the acylation of anisole compared to typical Al-MWW as well as Al-IEZ-MWW directly prepared under acidic conditions. The change in the state of Al atoms during the preparation process was investigated by high-resolution solid-state ^{27}Al MAS NMR and ^{27}Al MQMAS NMR techniques.

1. Introduction

Zeolites have been utilized in many industrial technologies, including gas adsorption, ion exchange, separation and catalysis for their unique porosity and high surface area [1, 2]. Recently, zeolites with more than 12-membered ring (12-MR) have received much attention because they can be used as effective catalysts for bulky reactant molecules which cannot enter into the micropores of 8 and 10 MRs [3, 4].

Zeolites with three-dimensional (3D) open framework structures are generally crystallized under hydrothermal conditions. In addition to this conventional route, the formation of 3D structures can be achieved by the structural conversion of a layered zeolitic precursor; layered zeolitic precursor is converted into a zeolite with 3D structures through topotactic dehydration-condensation of silanols on the precursor. For example, the layered precursors PREFER [5] and MCM-22(P) [6, 7] have been converted into ferrierite (**FER**) and MCM-22 (**MWW**), respectively. To date, various topotactic relationships between layered silicate material and the corresponding 3-dimensional zeolite crystals such as PLS-1 (PLS-4, RUB-36, MCM-47, MCM-65, UZM-13, UZM-17, and UZM-19) - CDS-1 (CDO), NU-6(1) - Nu-6(2) (NSI), EU-19(P) - EU-19 (CAS-NSI), RUB-39 - RUB-41 (RRO), RUB-18 - RUB-24 (RWR) and RUB-15 - sodalite (SOD) have been reported and summarized in excellent papers [8, 9].

Pillaring between interlayer spacings is a useful way of intercalating guest species between interlayer spacings of layered materials [10]. The interlayer spacings can be supported by pillars after being expanded through a suitable intercalation process. Furthermore, pillaring can provide new pores in addition to original micropores [10]. Based on the concept of “pillaring”, the periodic silylation using *e.g.* diethoxydimethylsilane (DEDMS) of the surface of layered silicates followed by connection between the interlayers leads to hierarchical structures consisting of two-types of pores, namely the original intralayer micropores and newly formed interlayer pores

[11-15].

We have developed a novel methodology of preparing an interlayer-expanded zeolite (IEZ) material through the interlayer silylation of layered zeolitic precursors such as MWW(P), PREFER, PLS-1 and MCM-47 [16-20]. Recently, interlayer-expanded **CDO**-type zeolites, COE-3 and COE-4, have been successfully prepared from layered RUB-36 [21-23]. Very recently, a top-down strategy that involves the disassembly of a parent layered zeolite, UTL, and its reassembly into two complex zeolites with targeted topologies, IPC-2 and IPC-4, has been developed [24].

In particular, treatment of the zeolitic layered precursor of Al-containing MWW, so-called Al-MWW(P), with DEDMS in acidic media leads to the formation of an aluminosilicate-type interlayer-expanded zeolite MWW (Al-IEZ-MWW) with expanded 12-membered ring (12-MR) micropores [17, 20]. In the silylation, acid, *e.g.*, HNO_3, enhances the extraction of the structure-directing agent (SDA) in the interlayer as well as the hydrolysis of the silylating agent followed by the condensation reaction of the silylating agent and the interlayer-silanol groups. Thus obtained Al-IEZ-MWW showed high catalytic activities for reactions involving bulky molecules due to the enlarged micropores between the layers via the interlayer-silylation [17, 19, 20].

Al-IEZ-MWW serves as a useful acid catalyst for the reaction of large molecules. However, the silylation process under acidic conditions simultaneously causes a dealumination from the **MWW** framework, resulting in the decrease in the acid amount [25]; the Si/Al atomic ratios of Al-MWW(P) and Al-IEZ-MWW were 15 and 35, respectively [17]. To suppress the dealumination, the vapor-phase silylation of Al-MWW(P) with dichlorodimethylsilane [20] and the preparation of Al-YNU-1 from deboronated MWW have been investigated [26]. Recently, we have developed the ‘‘two-step’’ silylation treatment with DEDMS via the first silylation in 0.1 M HNO_3 and the following silylation in 1.0 M NH_3 or water. This two-step silylation treatment successfully gave Al-IEZ-MWW that retains almost all the framework Al atoms [25].

Here we report a different method for preparing the Al-IEZ-MWW without leaching of the

Al species. The strategy is to conduct the silylation under weakly acidic conditions; the silylation was conducted in the aqueous solution of various ammonium salts instead of HNO_3. Furthermore, the combination of the silylation under weakly acidic conditions and the following acid treatment led to the formation of Al-IEZ-MWW with a high catalytic performance in the acylation of anisole compared to typical Al-MWW and Al-IEZ-MWW directly prepared under normal acidic conditions. In this study, to clarify the distribution of Al species in the MWW structure during the silylation followed by the acid treatment, ^{27}Al multiple quantum (MQ) MAS NMR technique [27] has been applied in addition to the high-resolution solid-state ^{27}Al magic angle spinning (MAS) NMR to investigate the change in the Al conditions during the preparation process.

2. Experimental

2.1. Preparation of Al-MWW layered precursor, Al-MWW(P)

The layered precursor of the **MWW**-type aluminosilicate, denoted by Al-MWW(P), was hydrothermally synthesized from fumed silica (SiO_2, Cab-O-Sil M5, Cabot), $NaAlO_2$ (33% Al_2O_3, 36.5% Na_2O, Kanto Chem.), NaOH (99%, Kanto Chem.), hexamethyleneimine (HMI, 99%, Kanto Chem.) and distilled water according to the literature with slight modifications [26]. The molar composition of initial gel was SiO_2: Al_2O_3: Na_2O: HMI: H_2O = 1.0 : 0.014: 0.075: 1.0: 45. After the hydrothermal crystallization at 150 ºC for 7 days, solid product, Al-MWW(P), was obtained by filtration followed by rinsing with distilled water and drying in an oven at 100 ºC overnight. The Si/Al ratio of the Al-MWW(P) was estimated at 27 by ICP measurement.

2.2. Interlayer silylation of Al-MWW(P)

The interlayer silylation of Al-MWW(P) was performed by using diethoxydimethylsilane ($Si(OEt)_2Me_2$, DEDMS) as a silylating agent under reflux conditions. The silylation was carried out in aqueous solution of 1.0 M ammonium salts such as NH_4NO_3, NH_4Cl, and CH_3COONH_4,

instead of 1.0 M HNO_3. The pH values of 1M NH_4NO_3, NH_4Cl and CH_3COONH_4 were 5.3, 5.0 and 7.0, respectively. Typically, 1.0 g of Al-MWW(P) was added to a mixture of 0.05 g of the silylating agent and 30 ml of aqueous solution of the 1.0 M ammonium salt and then the resulting mixture was stirred at 110 ºC under the reflux conditions for 24 h.. After the silylation, the solid was recovered by filtration followed by rinsing with distilled water and drying at 100 ºC. Thus obtained products were denoted by *e.g.*, Al-sil-MWW(P)-(NH_4Cl). As a control, the silylation was performed in water and aqueous solution of 1.0 M HNO_3, and the products were denoted by Al-sil-MWW(P)-(H_2O) and Al-sil-MWW(P)-(HNO_3), respectively. The silylated products were calcined at 550 ºC for 6 h to give the Al-IEZ-MWW samples, which was denoted by *e.g.*, Al-IEZ-MWW-(NH_4Cl) and Al-IEZ-MWW- (HNO_3). Conventional **MWW**-type aluminosilicate (denoted as Al-MWW) was also synthesized by calcination of Al-MWW(P) without the silylation treatment.

Besides, the acid treatment of the Al-IEZ-MWW samples prepared in the ammonium salts was conducted as follows: the sample was stirred at 80 ºC for 1 h in aqueous solution of HNO_3 with the pH varied in the range of 0.0 to 2.0. After the treatment, the solid was recovered by filtration followed by rinsing with distilled water and drying at 100 ºC. The acid-treated sample was denoted by *e.g.*, AT(pH1.0)-Al-IEZ-MWW(NH_4Cl).

2.3. Characterizations

The products were identified by X-ray diffraction (XRD, Ultima-III, Rigaku) using CuKa radiation at 40 kV and 20 mA. Nitrogen adsorption-desorption measurements to obtain information on the micro- and meso-porosities were conducted at -196 ºC K on a Belsorp-mini II (Bel Japan). The BET (Brunauer-Emmett-Teller) specific surface area (S_{BET}) was calculated from the adsorption data in the relative pressure ranging from 0.04 to 0.2. The micropore size distributions of the products were estimated by using argon adsorption at -186 ºC on an Autosorb-1 (Quantachrome Instrument). Prior to each adsorption measurement, the sample was evacuated at

200 ºC for 6 h.

Field-emission scanning electron microscopic (FE-SEM) images of the powder samples were obtained on an S-5200 (Hitachi) microscope operating at 1-30 kV. The samples for FE-SEM observations were mounted on a carbon-coated microgrid (Okenshoji) without any metal coating. Elemental analyses of the samples (Si/Al ratio) were performed on an inductively coupled plasma-atomic emission spectrometer (ICP-AES, Shimadzu ICPE-9000).

Temperature-programmed desorption of ammonia (NH_3-TPD) profiles were recorded on a BEL Japan Multitrack TPD equipment. Typically, 25 mg catalyst was pretreated at 600 ºC in He (50 mL min^{-1}) for 1 h and then was cooled to adsorption temperature of 373 K. Prior to the adsorption of NH_3, the sample was evacuated at 773 K. Approximately 2500 Pa of NH_3 was allowed to make contact with the sample for 10 min. Subsequently, the sample was evacuated to remove weakly adsorbed NH_3 for 30 min. Finally, the sample was heated from 373 to 873 K at a ramping rate of 10 K min^{-1} with a He flow (50 mL min^{-1}) passed through the reactor. A mass spectrometer was used to monitor desorbed NH_3 (m/e = 16). The amount of acid sites was determined by using the area of the so-called ‘‘h-peak’’ in the profiles [28].

The high-resolution ^{13}C CP-MAS, ^{29}Si MAS, ^{27}Al MAS NMR, and ^{27}Al 3Q MQMAS NMR spectra were obtained on a JEOL ECA-600 spectrometer (14.1 T) equipped with an additional 1 kW power amplifier. For ^{27}Al 3Q MQMAS NMR spectra, the 3Q excitation pulse and the 3Q-1Q conversion pulse were 5.5 and 2.1 μs, respectively, z-filter was 0.2 ms . The relaxation delay time was 10 ms. The ^{27}Al chemical shift was referenced to $AlNH_4(SO_4)_2 \cdot 12H_2O$ at -0.54 ppm and samples were spun at 17 kHz by using a 4 mm ZrO_2 rotor.

2.4. Catalytic reaction

The Friedel-Crafts acylation of anisole with acetic anhydride was carried out at 60 ºC in an oil bath with stirring. In a typical batch, catalyst (50 mg), anisole (50 mmol) and acetic anhydride (5 mmol) were employed. The reaction products were analyzed on a gas chromatograph (GC-2014,

Shimadzu) equipped with a DB-5 capillary column and an FID detector.

3. Results and discussion

3.1. Preparation of Al-IEZ-MWW

Figs. 1 (a) and (b) show the XRD patterns of Al-MWW(P) and the silylated products in various solutions of ammonium salts before and after calcination, respectively. The XRD pattern of Al-MWW(P) indicated the full crystallization of the layered precursor of the MWW structure after hydrothermal synthesis. With regard to the layered structure along the c direction, the 002 reflection of the precursor clearly appeared at 2θ = 6.42° (d_{002} = 13.8 Å). By the calcination of Al-MWW(P), this peak was shifted to 2θ = 7.05° (d_{002} = 12.5 Å), which overlapped with the 100 reflection peak at 2θ = 7.13°, as a result of the dehydration-condensation of silanols located on the MWW layers.

In the silylated products except Al-sil-MWW(P)-(H_2O), the interlayer-expanded structure was maintained after the silylation and the following calcination, regardless of the ammonium salts, as evidenced by the presence of the 002 reflection peak at 2θ = 6.51° (d_{002} = 13.6 Å). Although Al-sil-MWW(P)-(H_2O) possessed the 002 peak at 6.51°, it was shifted to higher angle (2θ = 7.05°) upon calcination; the interlayer-expanded structure was not obtained. The preservation of the interlayer-spacing in the IEZ-type samples is due to the condensation of DEDMS molecules with the silanols on the interstitial surface of the **MWW** sheets followed by the formation of monomeric silica struts. These results are in agreement with previous reports on interlayer-expanded zeolites derived from Al-MWW(P) [17-21]. Attempt to conduct the silylation in the pure water solution without any ammonium salts was unsuccessful, clearly indicating a hydrolysis of DEDMS did not proceed under the neutral conditions.

To confirm the formation of the interlayer-expanded structure, the micropore size distribution was measured based on the Horvath-Kawazoe (H-K) method using argon adsorption

isotherms. Fig. 2 shows the micropore size distributions of Al-MWW, Al-IEZ-MWW-(HNO_3) and Al-IEZ-MWW-(NH_4Cl). Al-MWW showed one peak at ca. 6.2 Å with a shoulder at ca. 7.0 Å, corresponding to intralayer and interlayer 10-MR micropores, respectively. In contrast, both Al-IEZ-MWW-(HNO_3) and Al-IEZ-MWW-(NH_4Cl) gave two distinct peaks at ca. 6.2 and 8.0 Å, indicating that the interlayer 10-MR pores were expanded through the interlayer silylation of Al-MWW(P). The difference in the size of the interlayer between conventional MWW and the IEZ-type samples estimated by the H-K method (ca. 1.0 Å) coincides with the difference in d_{002} value between them (1.1 Å).

In the ^{13}C CP/MAS NMR spectra of the Al-sil-MWW(P)-(HNO_3) and Al-sil-MWW(P)-(NH_4Cl) samples (Fig 3 (a)), a peak at 0 ppm was newly observed in addition to the peaks ranging from 20 to 60 ppm, which were assigned to the C species derived from hexamethyleneimine. This peak at 0 ppm can be assigned to the C atom derived from Si-<u>C</u> bond in DEDMS, $Si(OEt)_2(Me)_2$. Correspondingly, the Si atom of $\underline{Si}Me_2(OH)_{2-n}(OSi)_n$ derived from DEDMS was observed at -10 ppm in their solid-state ^{29}Si MAS NMR spectra (Fig. 3 (b)). These results imply the presence of the $SiMe_2(OSi)_2$ moiety between the MWW layers in both the Al-sil-MWW(P)-(HNO_3) and Al-sil-MWW(P)-(NH_4Cl) samples.

The removal of the HMI molecules was investigated by TG/DTA analysis; in the TG curves, the weight loss between 200 - 350 ºC is corresponding to the HMI molecules located at the interlayer. We found that the HMI molecules located at the interlayer were not completely removed during the silylation process, and that the degree of the removal was not significantly affected by the type of the solvents used. Considering that the IEZ-MWW products were successfully obtained, the residence HMI molecules would not affect the degree of the silylation process. NH_4^+ ions as well as the residence HMI molecules might play an important role in the silylation; they might be located in the interlayer spacings during the silylation, enhancing the accessibility of DEDMS molecules to silanol groups on MWW(P).

Table 1 summarizes the Si/Al atomic ratio, the acid amount based on the NH_3-TPD

profiles and the BET surface area of the calcined products. The silylation in 1.0 M HNO_3 followed by the calcination caused the Al leaching from Al-MWW(P); the Si/Al rations of Al-MWW(P) and Al-IEZ-MWW-(HNO_3) were estimated at 27 and 35, respectively. The leaching of the framework Al led to the decrease in the acid amount; the acid amounts of Al-MWW and Al-IEZ-MWW-(HNO_3) were estimated at 0.46 and 0.25 mmol·g^{-1}, respectively. In contrast, in the silylation in the aqueous solution of ammonium salts including NH_4NO_3, NH_4Cl and CH_3COONH_4, the Al leaching was suppressed; the Si/Al ratio was estimated at 27. However, the acid amounts of the IEZ-type products prepared in the ammonium salts were lower than that of Al-MWW. By ^{27}Al MAS NMR results, the IEZ-type products prepared in the ammonium salts exhibited a stronger peak at 0 ppm, which is due to extra-framework Al specie that cannot work as the acid site, compared to Al-MWW.

The IEZ-type samples have a higher BET surface area compared to the conventional 3D-structured MWW sample. For the IEZ-type samples, the use of ammonium salts led to the enlarged BET surface area compared to the use of 1M HNO_3; *e.g.*, the BET surface areas of Al-IEZ-MWW-(NH_4Cl) and Al-IEZ-MWW-(HNO_3) were found to be 490 and 407 $m^2 \cdot g^{-1}$, respectively. Furthermore, the relative peak area of the D^n peak ($\underline{Si}Me_2(OH)_{2-n}(OSi)_n$) in the ^{29}Si MAS NMR spectra of Al-IEZ-MWW-(NH_4Cl) was apparently higher than that of Al-IEZ-MWW-(HNO_3). These results suggest that the silylation degree of Al-IEZ-MWW-(NH_4Cl) was higher than that of Al-IEZ-MWW-(HNO_3). The weakly acidic conditions (pH = 5.0) would be more effective for the silylation reaction than the strongly acidic ones, which could enhance the undesirable self-condensation of DEDMS molecules.

Solid-state ^{27}Al MAS NMR technique was used to investigate the conditions of Al species in the **MWW** framework. In general, the peaks around 45-60 and 0 ppm are assigned to tetrahedrally coordinated Al species in the framework of zeolite and octahedrally coordinated Al species in the extra-framework of zeolite, respectively. The ^{27}Al MAS NMR spectra of Al-MWW(P) and Al-MWW are shown in Fig. 4 (a). Al-MWW(P) showed a main peak appearing

at ca. 56 ppm with a shoulder peak at ca. 49 ppm. However, a strong peak at 0 ppm appeared in the spectrum of Al-MWW, indicating that a part of the framework Al species were changed to extra-framework ones during the formation of the 3D structure through the dehydration-condensation of silanols located on the MWW layers by calcination. Furthermore, the MWW sample showed a new shoulder peak at 61 ppm in addition to the peaks at 49 and 56 ppm. The peak at 61 ppm would be due to the framework Al species located in interlayer 10MR micropores. Figs. 4 (b) and (c) shows the ^{27}Al MAS NMR spectra of Al-MWW(P) and the silylated samples before and after calcination. Although the silylation did not cause a significant change in the Al conditions regardless of the solvents, the following calcination resulted in the formation of the extra-framework Al species. The more detailed discussion on the Al conditions based on the ^{27}Al MQMAS NMR spectra is described below.

3.2. Catalytic performance of Al-IEZ-MWW

The catalytic performance of thus prepared samples was evaluated by the acylation of anisole with acetic anhydride (Fig. 5 and Table 1). All the IEZ-type samples exhibited a higher yield of *p*-methoxyacetophenone (*p*-MAP) compared to Al-MWW as a result of the enlarged micropores between the layers via the interlayer-silylation. These results are in agreement with previous reports on interlayer-expanded MWW zeolites [17-21]. Note that Al-IEZ-MWW-(HNO_3) gave the highest yield of *p*-MAP among the IEZ-type samples, while the acid amount in Al-IEZ-MWW-(HNO_3) (Si/Al = 35) was lower than that in the IEZ-type samples prepared under the weakly acidic conditions (Si/Al = 27). This is probably because not all of the Al species in the IEZ-type samples prepared under the weakly acidic conditions are utilized for the active site.

3.3. Effectiveness of acid treatment of Al-IEZ-MWW

The distribution of the Al species in the framework would be dependent on the preparation

conditions. Al-IEZ-MWW-(HNO_3) was prepared by the reaction of Al-MWW(P) with DEDMS in aqueous solution HNO_3 under reflux conditions, *i.e.*, this process involved the acid treatment with HNO_3 as well as the silylation with DEDMS. In contrast, Al-IEZ-MWW-(NH_4Cl) was prepared by the silylation only, not subjected to the acid treatment. It is considered that the acid treatment would play an important role in enhancing the catalytic performance. Therefore, the effect of the acid treatment for Al-IEZ-MWW-(NH_4Cl) on the catalytic performance was investigated.

Fig. 6 shows the XRD patterns of the Al-IEZ-MWW-(NH_4Cl) samples before and after the acid treatment with the pH varied in the range of 2.0 to 0.0. Thus treated samples were designated as *e.g.*, AT(pH1.0)-IEZ-MWW-(NH_4Cl). The presence of the 002 peak shows that the IEZ structure was retained even after the acid treatment regardless of the pH. There is no marked change in the BET surface area after the acid treatment (Table 2). Unfortunately, the acid treatment led to the dealumination; at the pH of 2.0, 1.5, 1.0, 0.5 and 0.0, the Si/Al ratios were estimated at 28, 29, 37, 54 and 78, respectively.

The ^{27}Al MAS NMR spectra of the acid treated Al-IEZ-MWW-(NH_4Cl) samples are shown in Fig. 7. When the pH of the acid treatment was decreased from 2.0 to 1.0, the intensities of the peaks at 40-60 ppm were not significantly changed but the peak at around 0 ppm was increased, indicating that the framework Al species were gradually transformed to extra-framework ones through the acid treatment. When the pH was further decreased to 0.0, the peak at around 0 ppm almost disappeared and the framework Al species were also decreased. The severe acid treatment resulted in the removal of the Al species both in the extra-framework and in the framework.

The Al-IEZ-MWW-(NH_4Cl) samples treated with highly acidic conditions, *i.e.*, AT(pH0)-Al-IEZ-MWW(NH_4Cl), AT(pH0.5)-Al-IEZ-MWW(NH_4Cl) and AT(pH1.0)-Al-IEZ-MWW(NH_4Cl) surpassed Al-IEZ-MWW-(HNO_3) as well as Al-IEZ-MWW-(NH_4Cl) in the catalytic performance (Fig. 8) despite of the low Al content compared to Al-IEZ-MWW-(HNO_3) (Si/Al = 35) and Al-IEZ-MWW-(NH_4Cl) (Si/Al = 27).

When the pH of the acid treatment was 0.5, the yield of *p*-MAP reached to 30% at the reaction time of 3 h. These results may suggest that the acid treatment led to a change in the distribution of Al species in the framework, forming catalytically active sites to improve the catalytic performance.

3.4. Distribution of Al species in the MWW framework

To date, high-resolution ^{27}Al MAS NMR and ^{27}Al MQMAS NMR techniques have been extensively applied to ZSM-5 [29-32], MCM-22 [33, 34], USY [35] and Beta [36] to obtain information about Al distribution in T sites. To clarify the change in the distribution of Al species in the **MWW** framework during the silylation and the calcination followed by the acid treatment, ^{27}Al multiple quantum (MQ) MAS NMR technique has been applied in addition to the solid-state ^{27}Al MAS NMR technique. Very recently, we have clarified the distribution of Al in the **RTH**-type framework by the ^{27}Al MQMAS NMR [37].

The ^{27}Al 3Q MQMAS NMR spectra of the representative samples are shown in Fig 9. The axis F1 in the MQMAS NMR spectra after an appropriate shearing consists of isotropic lines accompanied by second-order quadrupolar shifts for the central transition with their respective anisotropic quadrupolar features on the axis F2 [27]. Although quantitative discussion on the Al species is difficult, the number of cross-sections in the MQMAS NMR spectrum allows us to estimate the distribution of Al species.

Three cross-sections indicated by the arrows A - C were observed in the spectrum of Al-MWW (Fig 9(a)); at least three crystallographically distinct Al species, which were designated as Al_A, Al_B and Al_C were present in Al-MWW and the proportion of Al_A was the highest among these three species.

The **MWW**-type zeolite has 8 type T-sites (T1-T8) with different mean T-O-T angles ranging from 143 to 162° (Scheme 1) [38, 39]. In the ^{27}Al MAS NMR spectrum of the **MWW**-type aluminosilicate zeolite, the Al atoms corresponding to the peaks at 49 and 56 ppm are ascribed to the T6 and T7 sites and the T1, T3 T4, T5 and T8 sites in the hexagonal model,

respectively. The Al atom corresponding to the peak at 61 ppm is ascribed to the T2 site. Based on the projection lines on the axis F1, the framework Al_A, Al_B and Al_C species are ascribed to T6 and T7 sites, the T1, T3 T4, T5 and T8 sites and T2 site, respectively.

After the silylation in the aqueous solution of 1 M HNO_3 followed by the calcination (Al-IEZ-MWW-(HNO_3)), the cross-sections indicated by the arrows A and B were observed but the cross section C (T2 site) was hardly observed compared to Al-MWW. The silylation process under acidic conditions simultaneously causes a dealumination from the **MWW** framework; the Si/Al ratio was changed from 27 to 35. Hence, the framework Al_C atom specie might have been preferentially removed; the Al atoms located at the T2 site could be less resistant to the strongly acidic conditions than those at other sites.

Note that, the cross-sections indicated by the arrows D, E and F (these Al species were designated as Al_D, Al_E and Al_F) were newly observed in the spectrum of Al-IEZ-MWW-(HNO_3) (Fig. 9 (b). These changes should be due to the interlayer-expansion. The framework Al_D and Al_F species would be related to the framework Al_A, which are ascribed to T1, T3 T4, T5 and T8 sites and the framework Al_E specie would be related to Al_B, which are ascribed to T6 and T7 sites.

Unlike Al-IEZ-MWW-(HNO_3), the cross section C was observed in the spectrum of Al-IEZ-MWW-(NH_4Cl). The additional formation of the cross-sections D, E and F (Fig. 9 (c)) was also observed, being similar to the case of Al-IEZ-MWW-(HNO_3). For AT(pH1.0)-Al-IEZ-MWW(NH_4Cl), the cross-section F almost disappeared with the cross-sections D and E intact, and the cross-section C was still retained though noises were observed in the spectrum (Fig. 9 (d)). It is considered that the Al atoms located at the T2 site could be less resistant to the “strongly” acidic conditions than those at other sites, and that, the amount of the Al atoms located at the T2 site in Al-IEZ-MWW-(NH_4Cl) was relatively higher than that in Al-IEZ-MWW-(HNO_3), resulting in the slight preservation of the cross section C even after the subsequent acid treatment.

The acid treatment caused the dealumination; the Si/Al ratio was increased from 27 to 37,

while the extra-framework Al species were not removed (Fig. 7 (f)). These facts suggested that the framework Al_F specie was preferentially removed during the acid treatment. The framework Al_F atom might be much less resistant to the acidic conditions compared to the framework Al_C. Considering that AT(pH1.0)-Al-IEZ-MWW(NH_4Cl) exhibited a higher catalytic performance compared to Al-IEZ-MWW-(NH_4Cl) as well as Al-IEZ-MWW-(HNO_3) and Al-MWW (Fig. 8), it is considered that the framework Al_F would not contribute to the active site. Al-IEZ-MWW-(HNO_3) contained the framework Al_F, while the framework Al_C was nearly lost. This is the reason why Al-IEZ-MWW-(HNO_3) exhibited a lower catalytic performance than AT(pH1.0)-Al-IEZ-MWW(NH_4Cl). It is concluded that the change in the Al distribution in the framework as well as the interlayer-expanded structure would be the factors behind the change in the catalytic performance, and that the change in the Al distribution is strongly affected the treatment conditions. The attribution of each cross-section in the ^{27}Al MQMAS NMR spectrum to a specific T site and the clarification of the relationship between Al distribution and catalytic performance are still under investigation; the distribution of Al atoms is further investigated by applying *e.g.*, ^{29}Si and ^{27}Al double-quantum (DQ) MAS NMR [40] and ^{27}Al-^{29}Si_heteronuclear correlation (HETCOR) NMR techniques [41].

4. Conclusions

Al-IEZ-MWW was successfully prepared via the interlayer-silylation in the aqueous solution of ammonium salt instead of HNO_3. This method improved the degree of the interlayer-silylation with the leaching of the Al completely suppressed. Unfortunately, thus prepared Al-IEZ-MWW-(NH_4Cl) did not exhibit a superior catalytic performance in the acylation of anisole. However, subsequent acid treatment with aqueous solution of 0.5 - 1 M HNO_3 led to the dramatic improvement in the catalytic performance though the content of Al was decreased to some extent. ^{27}Al MQMAS NMR techniques is found to be a useful technique for clarifying crystallographically distinct Al species in the **MWW** framework; the combination of the interlayer-silylation in the aqueous solution of ammonium salt and subsequent acid treatment led to

the formation of the framework Al species that can effectively work as the active site for the acylation. Thus developed method is a promising method for preparing useful acid catalysts possessing large micropores and effective acid sites.

References

[1] C. S. Cundy, P. A. Cox, Chem. Rev. 103 (2003) 663-702
[2] A. Corma, J. Catal. 216 (2003) 298-312
[3] M.E. Davis, Chem. Eur. J. 3 (1997) 1745.
[4] M.E. Davis, Nature 417 (2002) 813.
[5] L. Schreyeck, P. Caullet, J.C. Mougenel, J.-L. Guth, B. Marler, Micropor. Mater. 6 (1996) 259.
[6] M. Rubin, P. Chu, US Patent 4, 954, 325, 1990.
[7] M.E. Leonowicz, J.A. Lawton, S.L. Lawton, M.K. Rubin, Science 264 (1994) 1910.
[8] Roth, W. J.; Čejka, J. Catal. Sci. Technol., 1 (2011) 43-53.
[9] B. Marler and H. Gies, European Journal of Mineralogy, 24 (2012) 405-428.
[10] M. Tsapatsis, S. Maheshwari, Angew. Chem., Int. Ed., 47 (2008) 4262.
[11] D. Mochizuki, A. Shimojima, T. Imagawa, K. Kuroda, J. Am. Chem. Soc. 127 (2005) 7183.
[12] D. Mochizuki, K. Kuroda, New J. Chem. 30 (2006) 277.
[13] D. Mochizuki, S. Kowata, K. Kuroda, Chem. Mater. 18 (2006) 5223.
[14] R. Ishii, T. Ikeda, T. Itoh, T. Ebina, T. Yokoyama, T. Hanaoka, F. Mizukami, J. Mater. Chem. 16 (2006) 4035.
[15] R. Ishii, T. Ikeda, F. Mizukami, J. Colloid Interface Sci. 331 (2009) 417.
[16] S. Inagaki, T. Yokoi, Y. Kubota, T. Tatsumi, Chem. Commun. (2007) 5188.
[17] P. Wu, J. Ruan, L. Wang, L. Wu, Y. Wang, Y. Liu, W. Fan, M. He, O. Terasaki, T. Tatsumi, J. Am. Chem. Soc. 130 (2008) 8178.
[18] J. Ruan, P. Wu, B. Slater, Z. Zhao, L. Wu, O. Terasaki, Chem. Mater. 21 (2009) 2904.
[19] L. Wang, Y. Wang, Y. Liu, H. Wu, X. Li, M. He, P. Wu, J. Mater. Chem. 19 (2009) 8594.
[20] S. Inagaki, T. Tatsumi, Chem. Commun. (2009) 2583.
[21] F.-S. Xiao, B. Xie, H. Zhang, L. Wang, X. Meng, W. Zhang,. X. Bao, Yilmaz, U. Müller, ChemCatChem, 3 (2011)1442 – 1446.
[22] H. Gies, U. Müller, B. Yilmaz, M. Feyen, T. Tatsumi, H. Imai, H. Zhang, B. Xie, F.-S. Xiao, X. Bao, W. Zhang, T. De Baerdemaeker, D. De Vos, Chem. Mater. 24 (2012) 1536−1545
[23] Z. Zhao, W. Zhang,. P. Ren,. X. Han, U. Müller, B. Yilmaz, M. Feyen, H. Gies, F.-S. Xiao, D. De Vos, T. Tatsumi, X. Bao, Chem. Mater. 25 (2013) 840−847.
[24] W. J. Roth, P. Nachtigall, R. E. Morris, P. S. Wheatley, V. R. Seymour, S. E. Ashbrook, P. Chlubná, L. Grajciar, M. Položij, A. Zukal, O. Shvets, J. Čejka, Nature Chem. 5 (2013) 628-633.

[25] S. Inagaki, H. Imai, S. Tsujiuchi, H. Yakushiji, T. Yokoi, T. Tatsumi, Micropor. Mesopor. Mater. 142 (2011) 354.

[26] W. Fan, S. Wei, T. Yokoi, S. Inagaki, J. Li, J. Wang, J.N. Kondo, T. Tatsumi, J. Catal. 266 (2009) 268.

[27] A. Medek, J. S. Harwood, L. Frydman, J. Am. Chem. Soc., 117 (1995) 12779.

[28] M. Niwa, K. Katada, Catal. Surv. Jpn. 1 (1997) 215.

[29] A. P. M. Kentgens, D. Iuga, M. Kalwei, H. Koller, J. Am. Chem. Soc. 123 (2001) 2925.

[30] P. Sarv, C. Fernandez, J.-P. Amoureux, K. Keskinen, J. Phys. Chem. 100 (1996) 19223.

[31] O. H. Han, C.-S. Kim, S. B. Hong, Angew. Chem. Int. Ed. 41 (2002) 469.

[32] S. Sklenak, J. Dedecek, C. Li, B. Wichterlová, V. Gábová, M. Sierka, J. Sauer, Angew. Chem. Int. Ed. 46 (2007) 7286.

[33] D. Ma, X. Han., S. Xie, X. Bao, H. Hu, S. C. F. Au-Yeung, Chem. Eur. J. 8 (2002) 162.

[34] A. Zheng, L. Chen, J. Yang, M. Zhang, Y. Su, Y. Yue, C. Ye, F. Deng J. Phys. Chem. B 109 (2005) 24273.

[35] N. Katada, S. Nakata, S. Kato, K. Kanehashi, K. Saito, M. Niwa, J. Mol. Catal. A, 236 (2005) 239.

[36] J. A. van Bokhoven, D. C. Koningsberger, P. Kunkeler, H. van Bekkum, A. P. M. Kentgens, J. Am. Chem. Soc. 122 (2000) 12842.

[37] M. Liu, T. Yokoi, M. Yoshioka, H. Imai, J. N. Kondo, T. Tatsumi, Phys. Chem. Chem. Phys., DOI:10.1039/C3CP54297A.

[38] S. L. Lawton, A. S. Fung, G. J. Kennedy, L. B. Alemany, C. D. Chang, G. H. Hatzikos, D. N. Lissy, M. K. Rubin, H. C. Timken, S. Steuernagel, D. E. Woessner, J. Phys. Chem. 100 (1996) 3788-3798.

[39] G. Sastre, V. Fornes, A. Corma, J. Phys. Chem. B 104 (2000) 4349-4354.

[40] D. H. Brouwer, P. E. Kristiansen, C. A. Fyfe, M. H. Levitt, J. Am. Chem. Soc., 127 (2005) 542-543.

[41] G. J. Kennedy, J. W. Wiench, M. Pruski, Stud Surf Sci Catal 174 (2008) 769-774.

Table 1

Structural properties and catalytic performances of Al-MWW and various IEZ-type samples

	Si/Al[*1]	Acid amount[*2] [mmol/g]	S_{BET}[*3] [m^2/g]	Yield of *p*-MAP[*4] [%]
Al-MWW	27	0.46	381	10
Al-IEZ-MWW (HNO_3)	35	0.25	407	23
Al-IEZ-MWW (NH_4NO_3)	27	0.35	505	15
Al-IEZ-MWW (NH_4Cl)	27	0.40	490	19
Al-IEZ-MWW (CH_3COONH_4)	27	0.41	460	12

[*1]: estimated by ICP measurement
[*2]: estimated by NH_3-TPD measurement
[*3]: BET surface area
[*4]: Reaction time of 3h

Table 2

Structural properties and catalytic performances of the Al-IEZ-MWW-(NH_4Cl) samples before and after the acid treatment with the pH varied

	Si/Al[*1]	Acid amount[*2] [mmol/g]	S_{BET}[*3] [m^2/g]	Yield of *p*-MAP[*4] [%]
Al-IEZ-MWW (NH_4Cl)	27	0.40	490	19
AT(pH2.0)-Al-IEZ-MWW (NH_4Cl)	28	0.39	462	19
AT(pH1.5)-Al-IEZ-MWW (NH_4Cl)	29	0.37	469	23
AT(pH1.0)-Al-IEZ-MWW (NH_4Cl)	37	0.33	504	29
AT(pH0.5)-Al-IEZ-MWW (NH_4Cl)	54	0.27	472	30
AT(pH0.0)-Al-IEZ-MWW (NH_4Cl)	78	0.16	460	25

[*1]: estimated by ICP measurement
[*2]: estimated by NH_3-TPD measurement
[*3]: BET surface area
[*4]: Reaction time of 3h

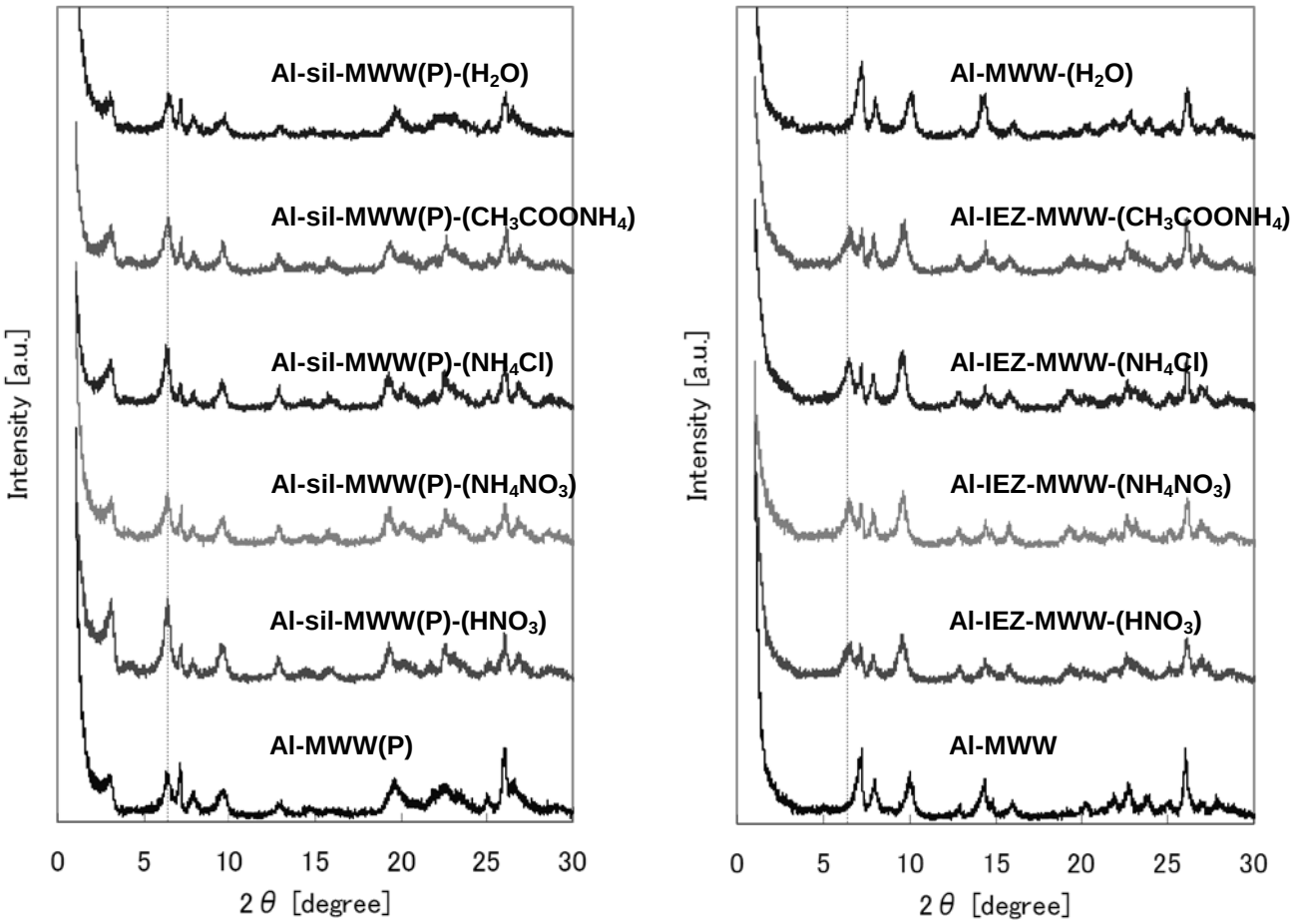

(a) (b)

Figs. 1 (a) and (b)

XRD patterns of Al-MWW(P) and the silylated products in various solutions (a) before and (b) after calcination.

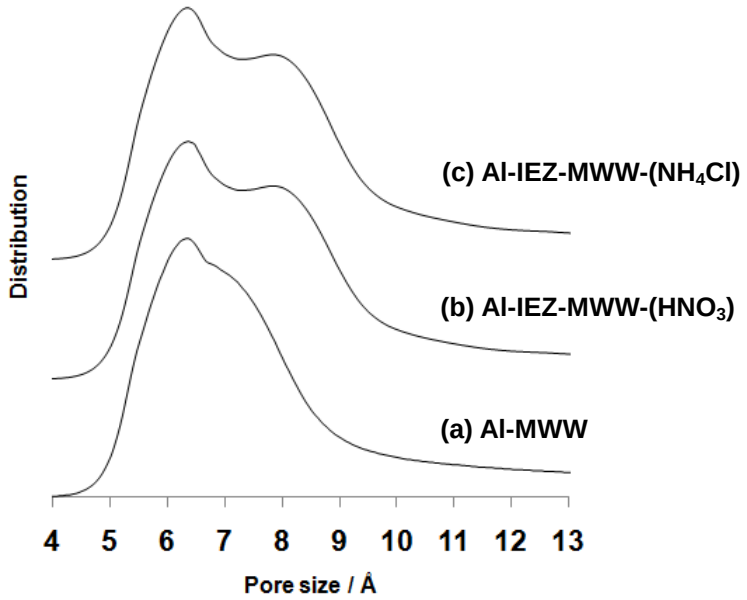

Fig. 2

Pore size distributions based on Ar adsorption isotherms. (a) Al-MWW, (b) Al-IEZ-MWW-(HNO_3) and (c) Al-IEZ-MWW-(NH_4Cl).

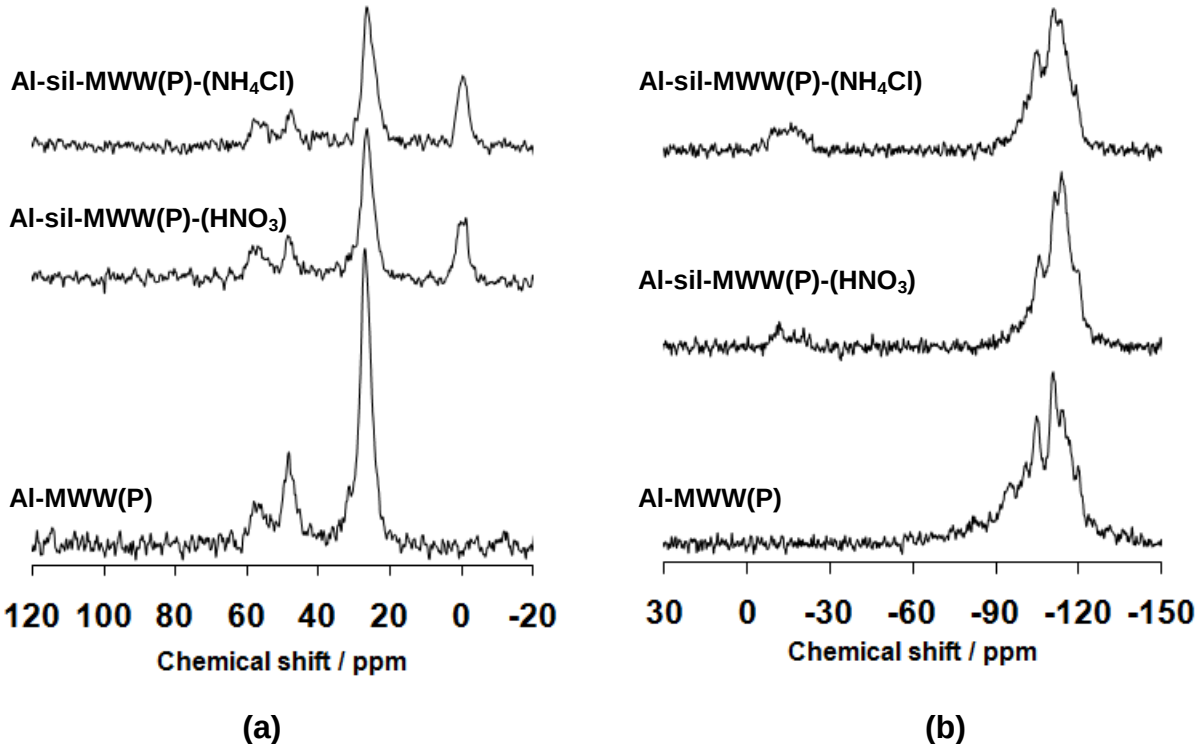

Figs. 3 (a) and (b)

(a) ^{13}C CP/MAS and (b) ^{29}Si MAS NMR spectra of Al-MWW(P), Al-sil-MWW(P)-(HNO_3) andAl-sil-MWW(P)-(NH_4Cl), respectively.

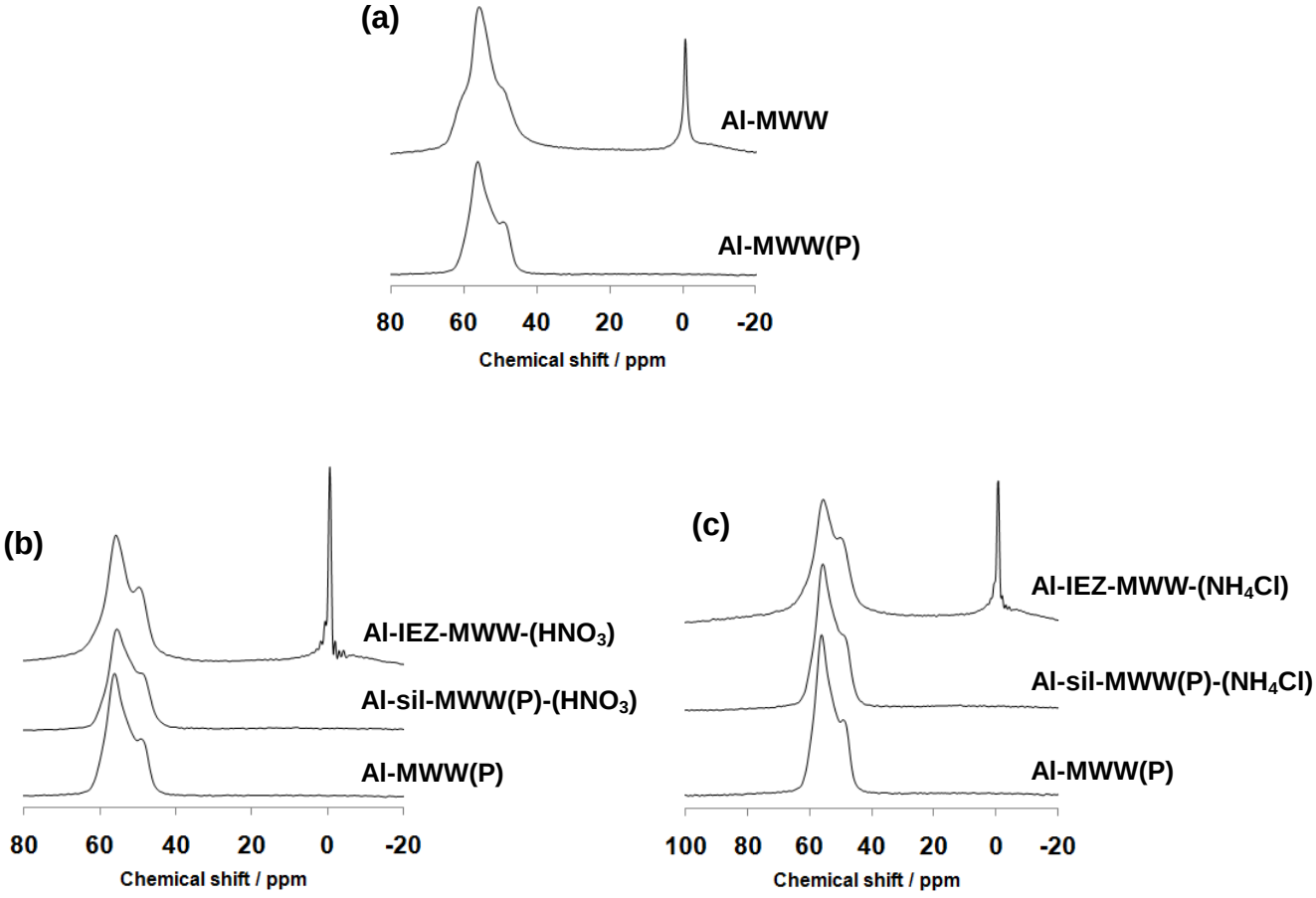

Figs. 4 (a), (b) and (c)

^{27}Al MAS NMR spectra of the representative samples before and after silylation and the following calcination.

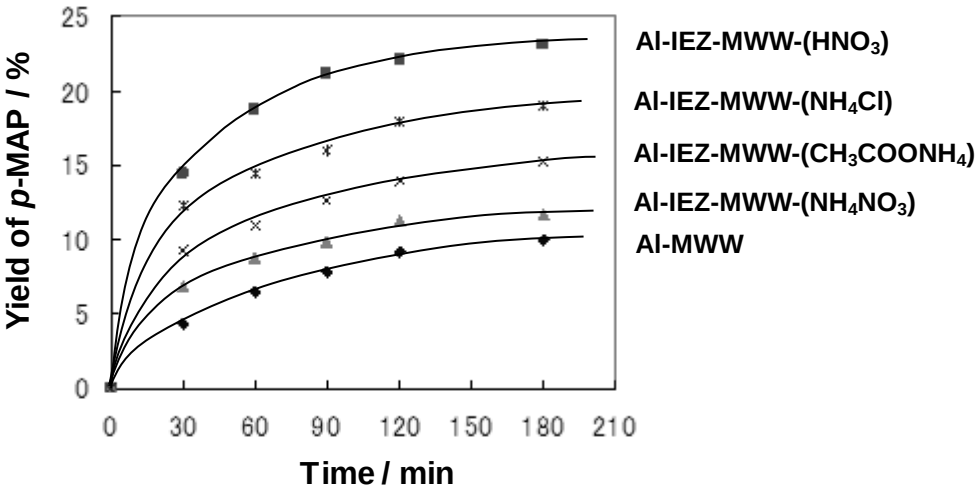

Fig. 5

Acylation of anisole with acetic anhydride over Al-MWW and various IEZ-type samples. Reaction conditions: catalyst., 50 mg; anisole, 50 mmol; acetic anhydride,5mmol; temperature., 60 ºC.

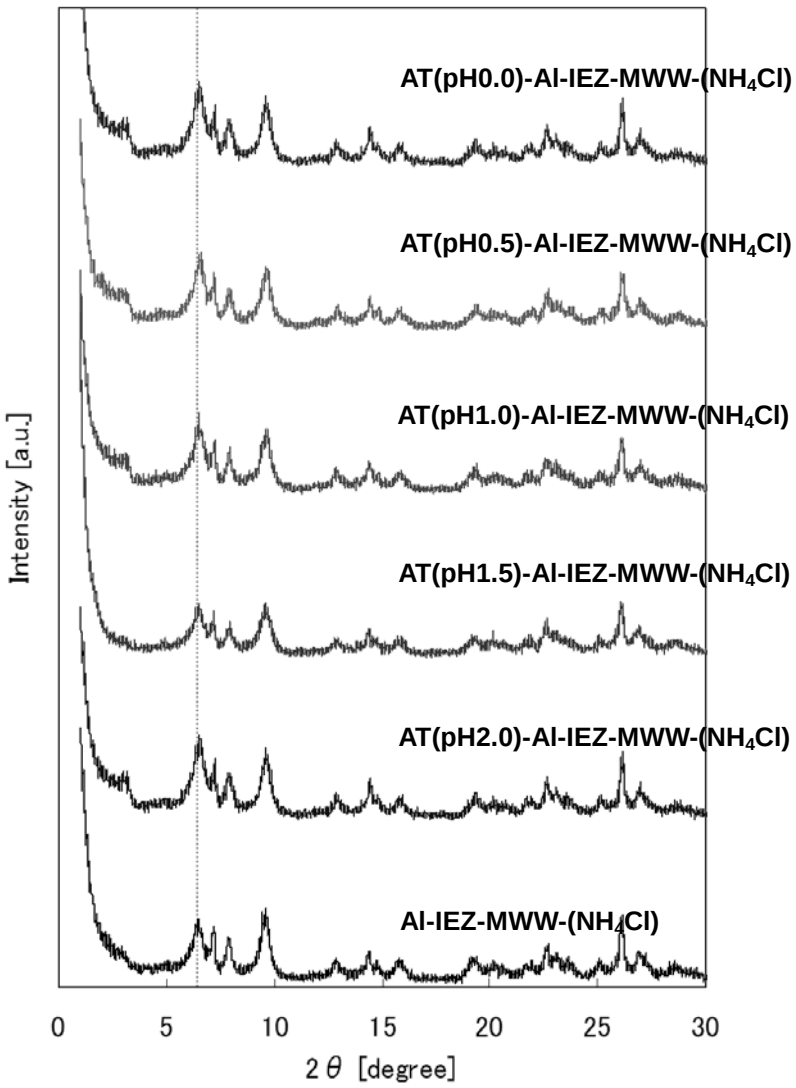

Fig. 6

XRD patterns of the Al-IEZ-MWW-(NH_4Cl) samples before and after the acid treatment with the pH varied ranging from 2.0 to 0.0.

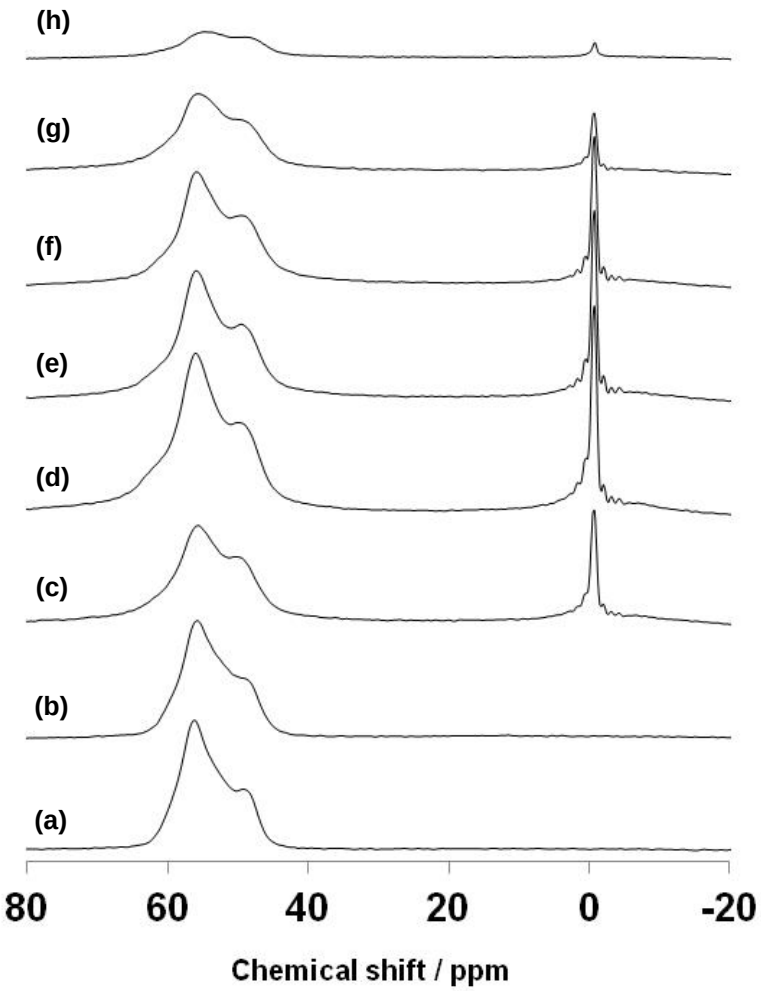

Fig. 7

^{27}Al MAS NMR spectra of Al-MWW(P), Al-sil-MWW(P)-(NH_4Cl) and the Al-IEZ-MWW-(NH_4Cl) samples before and after the acid treatment with the pH varied ranging from 2.0 to 0.0. (a) Al-MWW(P), (b) Al-sil-MWW(P)-(NH_4Cl), (c) Al-IEZ-MWW-(NH_4Cl), (d) AT(pH2.0)-, (e) AT(pH1.5)-, (f) AT(pH1.0)-, (g) AT(pH0.5)- and (h) AT(pH0.0)-Al-IEZ-MWW-(NH_4Cl).

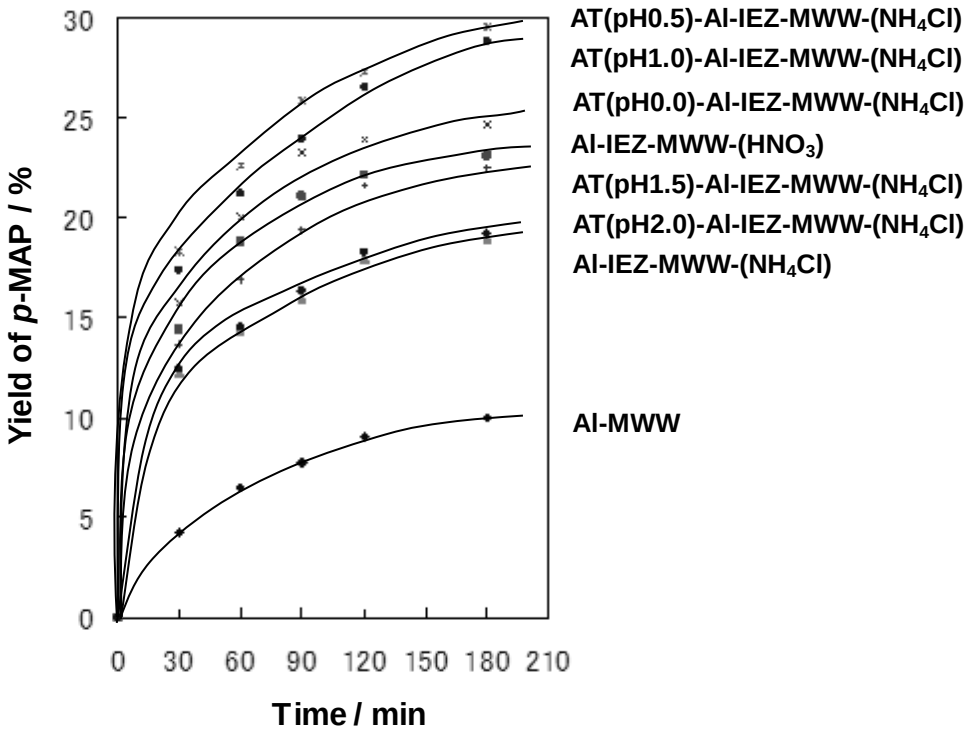

Fig. 8

Acylation of anisole with acetic anhydride over Al-MWW, Al-IEZ-MWW-(HNO_3) and the Al-IEZ-MWW-(NH_4Cl) samples before and after the acid treatment with the pH varied ranging from 2.0 to 0.0.

Reaction conditions: catalyst, 50 mg; anisole, 50 mmol; acetic anhydride,5mmol; temperature., 60 ºC.

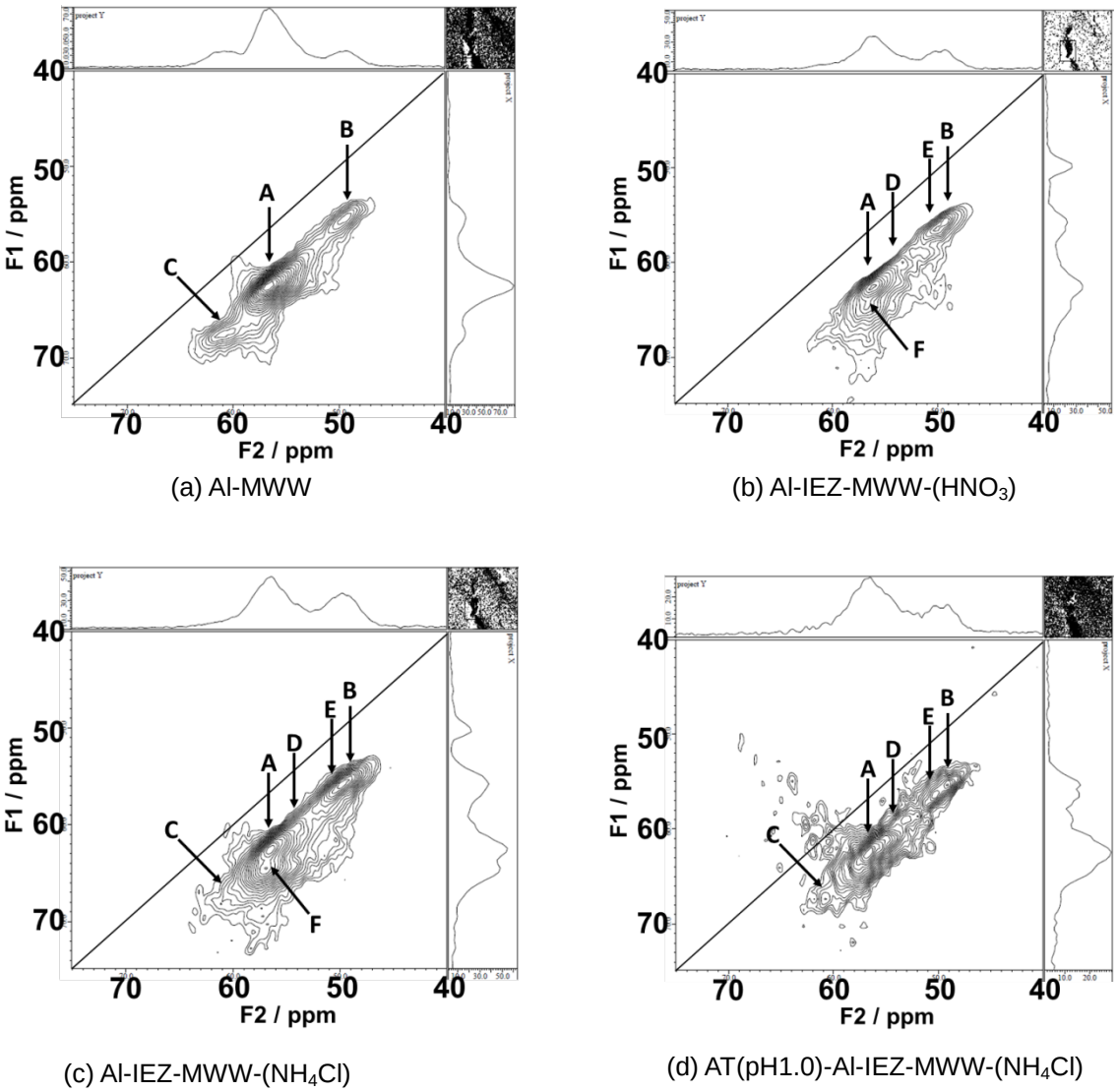

(a) Al-MWW

(b) Al-IEZ-MWW-(HNO_3)

(c) Al-IEZ-MWW-(NH_4Cl)

(d) AT(pH1.0)-Al-IEZ-MWW-(NH_4Cl)

Fig. 9

^{27}Al 3Q MQMAS NMR spectra of (a) Al-MWW, (b) Al-IEZ-MWW-(HNO_3), (c) Al-IEZ-MWW-(NH_4Cl) and (d) AT(pH1.0)-Al-IEZ-MWW-(NH_4Cl).

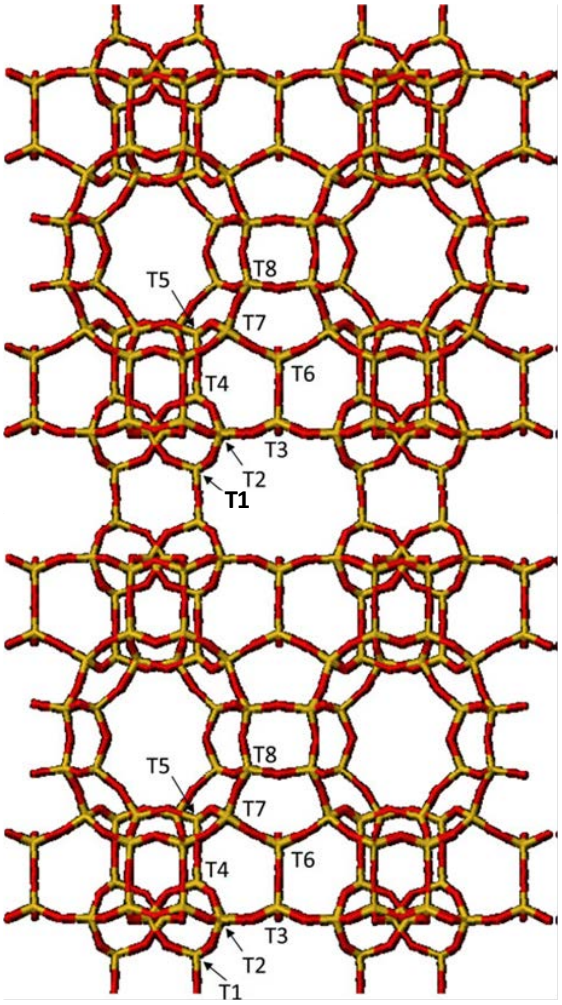

Scheme 1. Structure model of MCM-22 showing the eight crystallographically inequivalent T sites, only T atoms are shown.

Graphical abstract

Synthesis and structural characterization of Al-containing interlayer-expanded-MWW zeolite with high catalytic performance

Toshiyuki Yokoi, Shun Mizuno, Hiroyuki Imai, and Takashi Tasumi

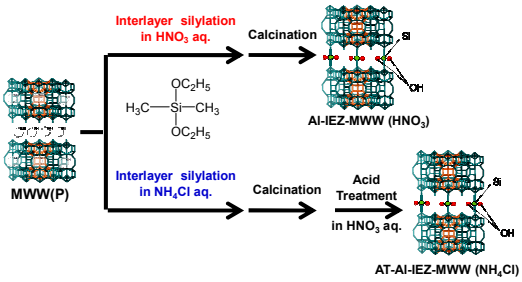

Al-IEZ-MWW was successfully prepared via the interlayer-silylation in the aqueous solution of ammonium salt instead of HNO_3.